



OPEN ACCESS

EDITED BY

Ting Zheng,
Hospital for Special Surgery, United States

REVIEWED BY

Koichi Murata,
Kyoto University, Japan
Vincenzo Ricci,
Luigi Sacco Hospital, Italy

*CORRESPONDENCE

Yuefeng Hao
✉ 13913109339@163.com
Xing Yang
✉ xingyangsz@126.com

RECEIVED 22 May 2024

ACCEPTED 25 July 2024

PUBLISHED 15 August 2024

CITATION

Zhang H, Ning E, Lu L, Zhou J, Shao Z, Yang X and Hao Y (2024) Research progress of ultrasound in accurate evaluation of cartilage injury in osteoarthritis. *Front. Endocrinol.* 15:1420049. doi: 10.3389/fendo.2024.1420049

COPYRIGHT

© 2024 Zhang, Ning, Lu, Zhou, Shao, Yang and Hao. This is an open-access article distributed under the terms of the [Creative Commons Attribution License \(CC BY\)](https://creativecommons.org/licenses/by/4.0/). The use, distribution or reproduction in other forums is permitted, provided the original author(s) and the copyright owner(s) are credited and that the original publication in this journal is cited, in accordance with accepted academic practice. No use, distribution or reproduction is permitted which does not comply with these terms.

Research progress of ultrasound in accurate evaluation of cartilage injury in osteoarthritis

Huili Zhang^{1,2}, Eryu Ning^{1,2}, Lingfeng Lu^{1,2}, Jing Zhou^{1,2}, Zhiqiang Shao¹, Xing Yang^{1,2*} and Yuefeng Hao^{1,2*}

¹Orthopedics and Sports Medicine Center, The Affiliated Suzhou Hospital of Nanjing Medical University, Suzhou, China, ²Gusu School, Nanjing Medical University, Suzhou, China

Osteoarthritis (OA) is a prevalent cause of joint algia, loss of function, and disability in adults, with cartilage injury being its core pathological manifestation. Since cartilage damage is non-renewable, the treatment outcome in the middle and late stages of OA is unsatisfactory, which can be minimized by changing lifestyle and other treatment modalities if diagnosed and managed in the early stages, indicating the importance of early diagnosis and monitoring of cartilage injury. Ultrasound technology has been used for timely diagnosis and even cartilage injury treatment, which is convenient and safe for the patient owing to no radiation exposure. Studies have demonstrated the effectiveness of ultrasound and its various quantitative ultrasound parameters, like ultrasound roughness index (URI), reflection coefficient (R), apparent integrated backscatter (AIB), thickness, and ultrasound elastography, in the early and accurate assessment of OA cartilage pathological changes, including surface and internal tissue, hardness, and thickness. Although many challenges are faced in the clinical application of this technology in diagnosis, ultrasound and ultrasound-assisted techniques offer a lot of promise for detecting early cartilage damage in OA. In this review, we have discussed the evaluation of ultrasonic cartilage quantitative parameters for early pathological cartilage changes.

KEYWORDS

cartilage, osteoarthritis, ultrasonography, knee joint, elasticity imaging techniques

1 Introduction

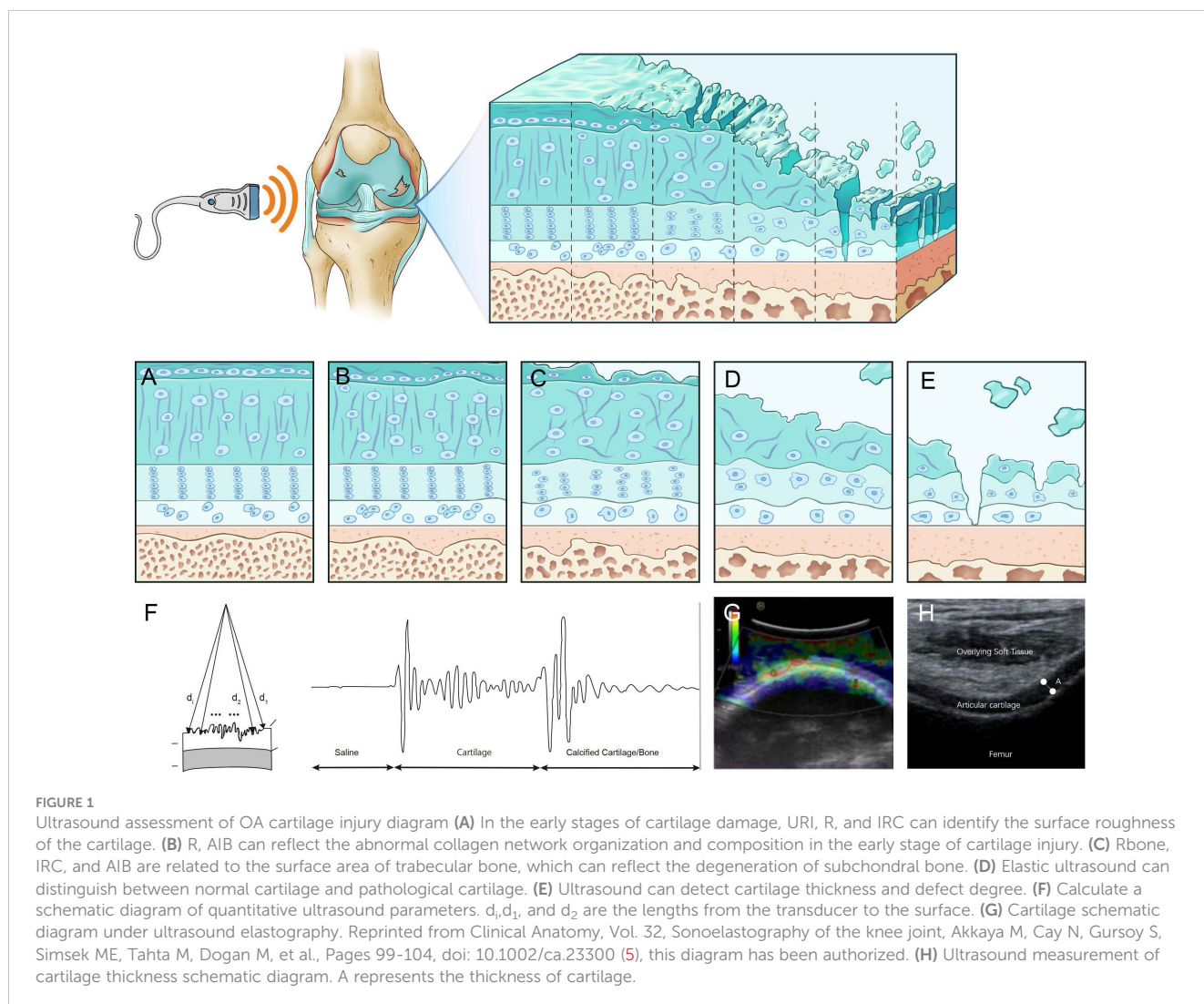
Osteoarthritis (OA) is a common and prevalent skeletal degenerative condition, where cartilage injury and degree of damage are regarded as the prime pathological changes incurred (1). Changes in the shape and structure of the cartilage surface and the components of cartilage in joints are essential symptoms and diagnostic bases for

Abbreviations: US, ultrasound; OA, osteoarthritis; URI, ultrasound roughness index; R, reflection coefficient; AIB, apparent integrated backscatter; TE, transient elastography.

evaluating cartilage injury. Additionally, the severity of cartilage injury is an essential reference for various scoring systems, including the International Cartilage Repair Society (ICRS). Applying cartilage repair treatments like self-chondrocyte implantation and self-osteochondral transplantation, as well as OA management medicines, necessitates a more accurate and objective evaluation of articular cartilage and subchondral bone integrity (2, 3). Therefore, accurate and sensitive evaluation of cartilage injury, real-time monitoring, changes in cartilage status assessment, and timely adoption of corresponding treatment measures are vital factors in OA diagnosis and treatment, which are pivotal for preventing late-stage complications (4) (Figure 1).

Ultrasound (US) is a safe, non-radiation, low-cost, and widely used technique for diagnosing musculoskeletal diseases and can give information about synovitis, joint effusion, periarticular soft tissues, and bony cortical abnormalities in peripheral OA joints (4, 6–8). Due to the high content of water and the absence of inner acoustic interfaces, the cartilage presents as hypoechoic or anechoic bands. Divided by two sharp hyperechoic interfaces of the cartilage-bone interface and synovial space-cartilage interface (9), the main

characteristics of healthy patient joint cartilage are low echo or anechoic and clear cartilage-bone interface and synovial fluid-cartilage interface. OA patients exhibit unevenly scattered echo bands on the surface or middle part of the tissue due to surface and internal degeneration such as decreased water content and fibrous degeneration. Mechanical damage results in joint cartilage damage and loss (Figure 2). Lately, studies have demonstrated that US-assisted technology can quantitatively detect cartilage changes and can disclose early cartilage pathologies or evaluate cartilage damage, which can measure cartilage thickness (6, 11, 12). In early osteoarthritis, the loss of proteoglycans and the destruction of surface collagen lead to fibrosis and softening of the soft bone surface (13, 14). Quantitative ultrasound parameters can provide information on surface fibrosis of articular cartilage, reflecting the destruction of surface collagen and the loss of proteoglycans, which helps to distinguish between normal and degenerative articular cartilage in the early stages of osteoarthritis (15, 16). Ultrasound elastography, as a new US imaging method, can detect articular cartilage softening before structural changes in knee osteoarthritis (KOA) and distinguish pathological cartilage from normal cartilage



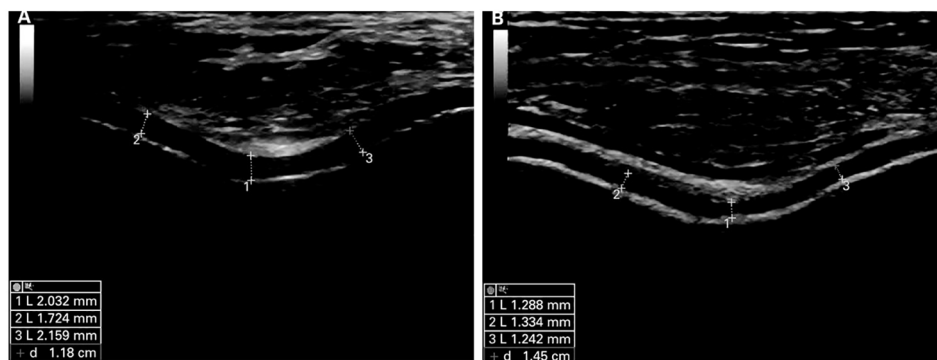


FIGURE 2 Ultrasound images of normal and damaged cartilage tissue in mode B. (A) is classified as normal cartilage. Articular cartilage shows hyperechoic, sharply defined interfaces. (B) is classified as pathological cartilage. Articular cartilage appears thinner and shows less defined interfaces. Reprinted from Annals of the Rheumatic Diseases, Vol. 68, Ultrasound Validity in the Measurement of Knee Cartilage Thickness, Naredo E, Acebes C, Moller I, Canillas F, de Agustin JJ, de Miguel E, et al., Pages 1322-1327, doi: 10.1136/ard.2008.090738 (10), this diagram has been authorized.

in the early stage of osteoarthritis (17, 18). It can detect changes in the hardness of articular cartilage before structural changes in knee osteoarthritis, which helps to achieve the goal of early diagnosis of OA. Cartilage thickness is an important indicator for describing the development and progression of osteoarthritis. Detecting cartilage thickness and the degree of cartilage damage is crucial for evaluating the progression and treatment response of OA (13, 19). Quantitative ultrasound parameters, ultrasound elastography, and ultrasound detection of soft bone thickness play a crucial role in the early diagnosis and treatment of OA and are crucial for preventing late complications and slowing down disease progression. Systematic articles on US-based evaluation of cartilage injuries still need to be included. This review aims to provide information about the US application in assessing OA cartilage injury and puts forward some suggestions for progress in this field.

2 Application of ultrasound in cartilage injury assessment

2.1 Quantitative ultrasound parameters have the potential to become measurement tools for the quantitative analysis of articular cartilage

The quantitative ultrasound parameters for evaluating cartilage injury assessment include the ultrasound roughness index (URI), reflection coefficient (R), cartilage-bone interface reflection coefficient (Rbone), apparent integrated backscatter (AIB), and integrated ultrasonic reflection coefficient (IRC). The early pathological manifestations of OA cartilage injury include surface fibrillation (13) and tissue swelling (14), due to the reduction in proteoglycan on the surface of cartilage in joints and the destruction of the surface collagen network. A study reported that the above-stated quantitative ultrasound parameters of cartilage could sensitively detect mechanical degeneration, roughness changes of the cartilage surface and spontaneous fibrous fibrillation, enzymatic

destruction of the surface collagen network, and degeneration of the subchondral bone, with an ability to distinguish between normal and degenerative articular cartilage in the initial stages of OA (Table 1).

The URI can monitor the cartilage surface microstructure and describe the morphological changes, where R and AIB of the cartilage surface are sensitive to the change in collagen content and structure. Similarly, R is also used to describe the characteristics of cartilage tissue (20), and cartilage surface R depicts the acoustic parameter in cartilage enzyme degradation (21). Furthermore, the AIB is sensitive to alterations in the number and direction of the collagen network (22); a drop in R and IRC, as well as a rise in URI, can diagnose enhanced cartilage surface roughness. Similarly, a decreased R and IRC on the cartilage surface also depicts enzyme-induced surface collagen network degeneration. Besides cartilage

TABLE 1 Measurement methods for partial quantitative ultrasound parameters reported in the literature.

Parameter	Equation
Ultrasound roughness index (13)	$URI = \sqrt{\frac{1}{m} \sum_{i=1}^m (d_i - \langle d \rangle)^2}$
Ultrasound reflection coefficient (14)	$R = \frac{1}{m} \sum_{i=1}^m \frac{A_{si}}{A_{iref}}$
Cartilage-bone interface reflection coefficient (14)	$R_{bone} = \frac{1}{m} \sum_{i=1}^m \frac{A_{bi}}{A_{iref}}$
Apparent integrated backscatter (13)	$AIB = \frac{1}{\Delta f} \int_{\Delta f} 10 \log_{10} \left\langle \frac{ A_b(f, z) ^2}{ A_0(f, z) ^2} \right\rangle df$
Integrated ultrasonic reflection coefficient (13)	$IRC = \frac{1}{\Delta f} \int_{\Delta f} 10 \log_{10} \left\langle \frac{ A_1(f, z) ^2}{ A_0(f, z) ^2} \right\rangle df$

m is the sample length's number of scan lines. di is the length from the transducer to the solution-cartilage boundary in the line i.⟨d⟩ is the average length from the transducer to the surface. The peak-to-peak amplitude of the ultrasonic RF signals that are reflected off the cartilage surface and the cartilage-bone contact, respectively, in line i is denoted by the letters Asi and Abi. Airef is the reference peak-to-peak amplitude measured from the solution-air interface at the same distance as Asi. Δf is the analyzed frequency range; Indices 0 and 1 refer to values obtained from the perfect reflector and sample, respectively. A(f, z) = amplitude spectrum of the pulse reflected at distance z from the transducer; Ab(f, z) = amplitude spectrum of the pulse backscattered at distance z from the transducer.

health assessment, US has also been shown to be sensitive to subchondral bone degeneration (23). The R and IRC of the cartilage-bone interface were significantly correlated with the trabecular bone's surface volume ratio and trabecular thickness. In the initial phases of OA, the bone around the joint is prone to change, including increased subchondral bone thickness, decreased subchondral trabecular bone mass, and the progression of calcified cartilage areas (24).

Moreover, quantitative ultrasound parameters are also helpful for accurately grading OA cartilage damage and viewing variations in the cartilage and internal tissues. Studies have demonstrated that increased URI is associated with an increased OA grade (14, 25, 26). With the progression of OA grading, the cartilage surface gets unequal and unpolished. Similarly, OA cartilage R decreases significantly compared to normal, whereas a decreased R significantly decreases with OA development. The increased surface roughness results in diffused reflection, reducing the echo amplitude (14). Additionally, with OA development, the cartilage softens, and the composition and framework of articular cartilage gradually change from the surface to the deep section. Since soft cartilage absorbs more transmission ultrasonic energy, the R-value decreases. As the OA stage increased, so did the R-value of the cartilage-bone interface, which was significantly higher than normal cartilage. Furthermore, the IRC was also strongly related to the early OARSI grade, where an increased IRC in OA was related to the R of the cartilage surface due to the destructive interference of incoherent waves scattered by surface fibrillation. An increased AIB might indicate abnormal organization and composition of the collagen network (16) since the AIB slope of early OARSI grading increased, whereas the AIB slope of degenerative cartilage samples was higher than that of healthy cartilage samples. The increased AIB slope in degenerated cartilage could be attributed to the collagen network rearrangement since the disorganized structure of diseased cartilage leads to greater backscatter than the deep vertical arrangement of fibers in normal cartilage (27).

The study reported that the cartilage surface R might be a more effective indicator than the URI and the cartilage-bone interface R to distinguish early OA grading (28). Many studies have also shown that the surface roughness index and R strongly correlate with the pathological evaluation of articular cartilage (14). In summary, quantitative ultrasound parameters can be used as a helpful assessment technique for quantitative articular cartilage assessment (14, 16, 29). They have also been applied for the quantitative diagnosis of cartilage lesions *in vivo* and *in vitro*, demonstrating the feasibility of *in vivo* US (Table 2).

2.2 Ultrasound elastography provides elastic information

2.2.1 The main classification and application of ultrasound elastography

The World Federation of Ultrasound Medicine and Biology has defined it as strain and shear wave imaging according to the measurement of elastography, where the former depicts tissue deformation when the probe exerts pressure on the tissue along

the propagation direction of the ultrasonic beam (including manual squeezing and acoustic radiation force pulse technique (ARFI)), while the latter is obtained by comparing the echo signals before and after compression (36). Strain imaging uses strain ratio to evaluate the deformation ability of tissue, where an increased strain ratio indicates softening, while acoustic elastography is based on shear wave technology (including transient elastography (TE) and ARFI), which excites the tissue to produce shear waves followed by measuring shear wave velocity. The hardness can be classified based on measuring the shear wave velocity, or Young's modulus. The ARFI method does not depend on the compression applied to the surface and can be used to evaluate deeper-position organs (37). Ultrasound elastography uses color maps to evaluate the tissue's deformability, where a change in color from blue to red indicates softening, overcoming the weakness of subjectivity of manual palpation, providing new elastic diagnostic information, expanding the scope of clinical application, could detect deep lesions and superficial masses, and has also been applied in cartilage injury (Table 3).

2.2.2 Application of ultrasound elastography in other diseases

Strain imaging has been applied for lesion detection in various tissues (39), such as the auxiliary diagnosis of thyroid nodules (40) and focal pancreatic lesions (41), and has unique advantages in the diagnosis of autoimmune pancreatitis (42). It can also be used to help identify acute and chronic deep vein thrombosis (43) and to assist in the identification of suspicious lymph nodes during lymph node puncture (44). Recent studies have found that strain elastography is also reliable for monitoring relative knee ligament stiffness (45). Sahan MH (46) used strain elastography to assist in measuring cartilage elasticity and evaluating variations in cartilage hardness in the initial phases of OA.

Shear wave imaging is mainly used to diagnose mild fibrosis or cirrhosis (47), and TE has mostly been utilized to assess liver stiffness measures (LSM) in individuals suffering from long-term viral hepatitis or additional illnesses, with more representative results of liver parenchymal stiffness compared to liver biopsy (39). The TE uses an external 'punching machine' with controllable vibration to produce shear waves, measure the average shear wave velocity in the region, and convert it into Young's modulus; hence, the TE standardization technique was specifically used for measuring liver tissue hardness rather than imaging (38). Shear wave elastography based on ARFI techniques can help diagnose the staging of liver fibrosis, detect and characterize focal liver lesions (48), and diagnose benign and malignant thyroid nodules (49), especially in the presence of chronic autoimmune thyroiditis (50). It has also been used for the gastrointestinal tract (51), heart (52), blood vessels, and musculoskeletal (53). Further, it can also be used to improve the accuracy of gastrointestinal tumor staging, assist in making a diagnosis of benign and malignant lymph nodes among individuals with primary cancer, improve the diagnosis of carotid plaque vulnerability (54), evaluate the directional mechanics of the heart and cartilage (52), quantify the mechanical properties of false

TABLE 2 Study on quantitative ultrasound parameters in measuring cartilage injury.

Authors	Material	Transducer frequency (MHz)	Anatomical site	n	Acquisition of ultrasonic parameters	Usage
Saarakkala S, Toyras J, et al. (20)	Mechanical degradation and enzymatic degradation of the bovine knee joint	20	Patella osteochondral specimens	44	URI, R, and IRC	Quantitative ultrasound imaging can detect collagen damage and an increase in the surface roughness of articular cartilage.
Viren T, Saarakkala S, et al. (30)	Surgical repair or spontaneous healing of rabbit knee joint tissue	40	Repair-site osteochondral specimens	13	URI, R, AIB, and IRC	Ultrasound can evaluate the surface integrity and internal structure of repaired tissues.
Viren T, Saarakkala S, et al. (31)	Mechanically degraded bovine knee joint specimens	40	Knee joint cartilage	7	URI, R, AIB, and IRC	Ultrasound can evaluate the integrity of the cartilage surface.
Niu HJ, Wang Q, et al. (14)	Rabbit knee cartilage specimens after ACL surgery	55	MFC, LFC, MTP, and LTP	18	URI, R, and Rbone	Ultrasound can detect changes in URI and R after an ACL operation.
Liukkonen J, Hirvasniemi J, et al. (23)	Cadaver specimens without a history of joint disease	9	FAC	13	URI, R, R _{bone} , AIB, and IRC	Ultrasound can evaluate the thickness and roughness of the cartilage surface.
Wang Q, Liu Z, et al. (32)	Rat knee joint cartilage	50	MFC, LFC, MTP, and LTP	14	URI, R	Ultrasound can detect the morphological and acoustic changes of knee joint cartilage.
Huang YP, Zhong J, et al. (33)	Total knee arthroplasty specimens of advanced knee osteoarthritis	25	Knee joint	10	URI, IRC	Ultrasound can measure the morphological changes at the junction of bone and cartilage.
Zhang J, Xiao L, et al. (34)	Porcine cartilage samples digested with trypsin and healthy control samples	15, 25	Porcine knee joint	36	IRC, AIB	Ultrasound can evaluate the integrity of the cartilage surface or the microstructure of the cartilage matrix.
Pastrama M, Spierings J, et al. (35)	Goats	31.25	Areas that articulate with the focal knee resurfacing implant and non-articulating areas	16	URI	Ultrasound can serve as a follow-up tool for evaluating cartilage quality.
Lye TH, Gachouch O, et al. (16)	Early human OA knee replacement specimens	40	MTP and LFC	26	AIB, IRC	Ultrasound can serve as a method for the early diagnosis and monitoring of osteoarthritis.

URI, ultrasound roughness index; R, ultrasound reflection coefficient; R_{bone}, cartilage-bone interface reflection coefficient; AIB, apparent integrated backscatter; IRC, integrated ultrasonic reflection coefficient; ACL, anterior cruciate ligament; MFC, medial femoral condyle; LFC, lateral femoral condyle; MTP, medial tibial plateau; LTP, lateral tibial plateau; FAC, femoral articular cartilage.

vocal cords in normal individuals, and evaluate the symmetry of false vocal cords (55). It also has the inherent advantage of diagnosing and treating neurological diseases such as Parkinson's disease (56), carpal tunnel syndrome (57), chronic stroke (58), and multiple sclerosis (59). Furthermore, it concentrates on the transverse waves created within the tissue, which can be employed for patients with ascites surrounding the liver and is more effective for obese people (60, 61).

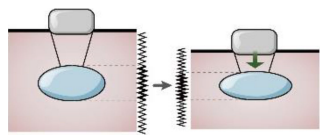
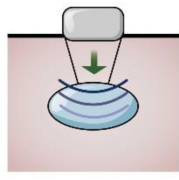
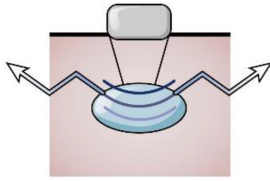
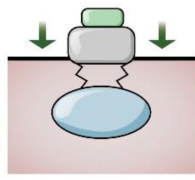
2.2.3 Ultrasound elastography distinguishes pathological cartilage from normal cartilage

The health and maintenance of articular cartilage highly depend on appropriate mechanical loading. In animal and human studies, both high loads and low physical activity have led to cartilage thinning and softening (62–64). Due to gravity forces, the body weight load may show different elastography features in normal and pathological conditions compared to the joints of the upper limb. The hardness of cartilage changes before cartilage structure changes

in the early stage of KOA (65); hence, it is important to evaluate cartilage elasticity (17). Strain elasticity imaging induces echo signal movement around the tissue, which the probe stresses to exert stable and regular pressure on the target tissue. The strain rate is obtained by contrasting the echo signals prior to and following pressure, where a higher strain (38) ensures more excellent material elasticity.

In a distal femoral cartilage evaluation study, real-time elastography was objectively used to evaluate tissue elasticity, where the diseased cartilage area's median strain value was substantially greater than healthy cartilage (5). Similarly, another study demonstrated that elastography might be an effective tool for displaying diseased cartilage and being used to distinguish diseased cartilage from normal cartilage (18), where the median strain value of the pathological femoral cartilage area was significantly higher than normal cartilage. In ultrasound elastography, blue coding of normal cartilage tissue shows typical echoless imaging characteristics, which are excellent clarity, devoid of focal defects,

TABLE 3 The calculation method of tissue stiffness is evaluated by elastography technology (38).

Measured physical quantity	Method	Type of elastography	Indicators	Schematic diagram
Strain or Displacement	Strain imaging	Strain elastography	Strain ratio E/B size ratio	
		Acoustic Radiation Force Impulse (ARFI) imaging	Displacement ratio E/B size ratio	
Shear wave speed	shear wave imaging	shear wave speed imaging	Shear wave speed (m/s) Young's modulus (kPa)	
		Transient elastography	Young's modulus (kPa)	

E/B size ratio (ratio of the size of a lesion in the strain image to its size in the B-mode image).

smooth bone surface, and unchanged thickness compared with adjacent tissues. In contrast, the pathological cartilage tissue coding showed irregular color changes from blue to red. In an event where US shows no difference in cartilage thickness, real-time elastography can be utilized to determine the change in cartilage hardness by calculating the strain ratio of the region. This technique can be used to forecast the degenerative changes in the knee joint after anterior cruciate ligament reconstruction (66). Shear wave elastography is a reliable, harmless, and acceptable technique for evaluating pathological cartilage (17, 67), where the shear wave value is correlated with the cartilage US score. The faster the shear wave speed or the greater Young's modulus, the lower the elasticity of the tissue and the higher the hardness. Different hardness levels can identify normal or abnormal tissues (36). Therefore, elastography can be used as an early detection method for evaluating OA cartilage injury (68).

2.3 Ultrasound is a reliable tool for quantifying cartilage thickness

For measuring cartilage thickness, US is a dependable, unbiased, and objective technology (6). It includes the measurement of the articular cartilage thickness of the knee, wrist, shoulder, and metacarpophalangeal joint. Measurement of early alterations in femoral cartilage thickness following ACL reconstruction helps

evaluate and prevent the occurrence of KOA (29). Articular cartilage thickness of metacarpophalangeal (MCP) and proximal interphalangeal (PIP) joints were measured to assist early identification and monitoring of bone erosion and cartilage injury in rheumatoid arthritis (69), as well as to measure the cartilage thickness of juvenile knee joint to assist the diagnosis of juvenile idiopathic arthritis (70). Prenatal US examination of fetal nasal soft tissue thickness and nasal bone length can effectively reduce the birth rate of fetuses with Down's syndrome, thus having high accuracy and clinical application value for screening fetuses with Down's syndrome (71, 72).

Due to mechanical damage, late-stage OA patients are characterized by joint cartilage damage, loss, and thinning of thickness. US recognition of changes in cartilage status is crucial for evaluating the effectiveness of strategies to reduce the risk of development and progression of KOA (4, 10). OA patients with cartilage defects face accelerated progression of OA (19) since cartilage thickness is an essential index for detecting the occurrence and development of OA, where detection and quantification of cartilage thickness and damage are crucial for evaluating OA's progression and treatment. The main characteristics of articular cartilage are hypochoic, anechoic, and clear cartilage bone and synovial cartilage interfaces. The high echo lines between the surface of the cartilage and synovial fluid are called "interface signs". Identifying the cartilage bone and synovial fluid cartilage interfaces is particularly important for measuring

TABLE 4 Study on the measurement of cartilage thickness by ultrasound.

Authors	Material	Transducer frequency (MHz)	Anatomical site	n	Studies	Conclusion
Yagi M, Taniguchi M, et al. (11)	OA patients	5- 18	MFC	22	22	Ultrasound can objectively and quantitatively evaluate early cartilage degeneration in osteoarthritis.
Okada S, Taniguchi M, et al. (81)			MFC	126	118	
Okada S, Taniguchi M, et al. (82)		44	MFC	56	34	
Lisee C, Harkey M, et al. (29)	Patients 4 to 6 months after ACLR	12	FAC	20	120	Ultrasound can diagnose thickening and thinning of femoral cartilage.
Pradsgaard DO, Fiirgaard B, et al. (70)	Children with JIA	6-14	FAC	23	138	Ultrasound can be consistent with MRI in measuring the average thickness of cartilage.
Printemps C, Cousin I, et al. (83)	4–12-week-old infants	8-10	Pubic cartilage	948	1896	Ultrasound can improve treatment decisions for hip dysplasia by measuring cartilage thickness.
Desai, P. Hacihaliloglu, I. et al. (6)	Healthy volunteers	8- 12	FAC	10	80	Ultrasound can objectively and effectively evaluate cartilage thickness.
Harkey MS, Blackburn JT, et al. (84)		12	MFC	25	75	
Devrimsel G, Beyazal MS, et al. (75)		7- 12	FAC	30	180	
Güvener O, Dağ F, et al. (12)		5-13	FAC	16	192	
Yildirim A, Onder ME, et al. (85)		7 - 12	FAC and talar cartilage	55	440	
Moller B, Bonel H, et al. (86)	RA patients	10 –15	MCP and PIP finger joint cartilage	48	1152	Ultrasound can distinguish early RA from healthy joints by reducing cartilage.
Yildirim A, Onder ME, et al. (85)		7 - 12	FAC and talar cartilage	55	440	
Kaya A, Kara M, et al. (87)	SLE patients	7- 12	FAC	29	174	Ultrasound can effectively and reliably evaluate the thickness of femoral cartilage in patients with systemic lupus erythematosus.
Güvener O, Dağ F, et al. (12)	Flatfoot patients	5-13	FAC	16	192	Ultrasound can measure the thickness of distal femoral cartilage in different conditions.
Naredo E, Acebes C, et al. (10)	Body knee specimens	14	FAC	8	24	Ultrasound can more accurately measure normal to moderately damaged cartilage.
Devrimsel G, Beyazal MS, et al. (75)	Patients with hypothyroidism	7- 12	FAC	40	240	Ultrasound can assist in the early diagnosis of osteoarthritis in patients with hypothyroidism.

MFC, medial femoral condyle; FAC, femoral articular cartilage; ACLR, anterior cruciate ligament reconstruction; JIA, juvenile idiopathic arthritis; MCP, metacarpophalangeal; PIP, proximal interphalangeal; RA, rheumatoid arthritis; SLE, systemic lupus erythematosus; US, ultrasound; MRI, magnetic resonance imaging.

cartilage thickness (9, 10). A significant number of studies in the literature suggest that US is a feasible clinical tool for assessing cartilage thickness, which has been found to be consistent with *in vitro* animal studies and autopsy thickness values and highly correlated with cartilage thickness measured by MRI (10, 73). Similarly, it was found *in vivo* that ultrasonography can

accurately measure cartilage thickness as well as the scope of damaged cartilage in the knee joint (74). Arthroscopic US can avoid bone occlusion in the joint and thoroughly evaluate the entire cartilage in the joint; in addition, it can accurately measure the thickness of the cartilage in the case of extremely thin cartilage, assessing the degree of regional cartilage damage relative to the

thickness of the entire articular cartilage (75). A significant correlation between US and arthroscopy has shown that US has an excellent predictive value in detecting the severity of cartilage degeneration and can also detect early pathological changes in articular cartilage.

Currently, the determination of cartilage thickness using US primarily relies on image segmentation or original radio frequency (RF) signal analysis. Although static US scans provide high-resolution and high-quality images, cartilage data analysis faces challenges due to low contrast, high-level speckle noise, and various imaging issues in US images. There is an urgent need for accurate, stable, and fully automated methods to enhance US images and segment cartilage, thus enhancing the widespread utility of US imaging techniques. Various technologies have been developed to address this need, including multipurpose beta-optimized recursive histogram equalization (MBORBHE), the random walker (RW) algorithm, the local statistical level set method (LSLSM), and deep learning methods (6, 76–78). For instance, MBORBHE is utilized to enhance cartilage regions in US images, preserving essential information such as brightness shifts and contrast enhancement. However, this method may inadvertently enhance the soft tissue interface, potentially affecting cartilage segmentation and thickness measurement. The RW algorithm is employed for automatic cartilage segmentation, although it is susceptible to changes in anatomical structure (6). Another approach involves using the LSLSM to segment cartilage from two-dimensional knee joint US data. While it yields promising results, post-processing of the segmented image using connected component labels is necessary (77). Deep learning frameworks, such as convolutional neural networks, are employed to regress the cartilage interface distance field, delineate cartilage interfaces, and calculate cartilage thickness (76). Furthermore, the original RF signal is tracked using peak detection algorithms to analyze surface displacement and calculate cartilage thickness (78). Active or passive movements during US evaluation can also be used to observe the flow of synovial fluid within focal cartilage defects that are almost invisible in static US imaging, significantly improving the sensitivity and specificity of the examination. ACL injury is a key risk factor for the development of KOA, and imaging of this ligament under static US is difficult, but dynamic US can help confirm structural lesions. Dynamic US can help better visualize and simulate different anatomical structures in daily life, which is helpful for the diagnosis of OA complications such as synovitis and joint effusion. It plays an increasingly important role in evaluating joint cartilage tissue (79, 80) (Table 4).

3 Conclusion and future perspectives

US has many characteristics that make it valuable in evaluating OA cartilage damage. Quantitative ultrasound parameters can detect early collagen fracture of articular cartilage and rough and uneven articular cartilage surfaces, which can be utilized to assess the integrity of articular cartilage and provide helpful information for quantitative ultrasound diagnosis of early OA. As a novel

ultrasonic imaging method, elastography is more promising than traditional US, where additional imaging can provide valuable information on articular cartilage elasticity to clinicians. Elastography also finds applications in determining tissue properties, structure, and function. Currently, it is shown in the initial rhinoplasty and revision nasal surgery that strain ultrasound elastography can assist in the selection of the correct tissue for cartilage transplantation. It is foreseeable that more advanced US technologies will continue to rapidly evolve in the coming years. US can accurately measure cartilage thickness, degree, and depth of cartilage defects, enhance accuracy in clinical OA classification, and improve and evaluate OA's progress and treatment response by detecting and monitoring the therapeutic effect of cartilage injury. In recent times, there has been a pervasive utilization of three-dimensional US imaging technology, addressing the constraints associated with two-dimensional imaging for the observation of cartilage's three-dimensional structure. This advancement facilitates comprehensive and volumetric cartilage imaging, furnishing practitioners with augmented data for precise morphological and functional assessments. Moreover, the ongoing evolution of artificial intelligence (AI) technology within the realm of US cartilage imaging, encompassing the training of deep learning models, holds promise for automating the analysis and diagnosis of cartilage imaging data, thereby enhancing diagnostic precision and workflow efficiency. US is a rapidly growing technology with enormous possibilities for future clinical applications. We have shown in our overview that US can be employed in basic studies of articular cartilage to evaluate early histopathology, elasticity, thickness, degree of changes, and defects in articular cartilage, which play a crucial role in detecting early bone and joint disorders. Although there are still many challenges in the development of US diagnostic tools, they play an increasingly important role in the diagnosis of cartilage injuries.

Author contributions

HZ: Writing – original draft. EN: Writing – review & editing. LL: Writing – review & editing. JZ: Writing – review & editing. ZS: Writing – review & editing. XY: Writing – review & editing. YH: Writing – review & editing.

Funding

The author(s) declare financial support was received for the research, authorship, and/or publication of this article. This work was funded by the Jiangsu Science and Technology Department (BK20211083, BE2022737), the Jiangsu Graduate Student Cultivation Innovative Engineering Graduate Research and Practice Innovation Program (SJCX23_0683), and the Suzhou Health Commission (GSWS2020078, SZXK202111).

Conflict of interest

The authors declare that the research was conducted in the absence of any commercial or financial relationships that could be construed as a potential conflict of interest.

Publisher's note

All claims expressed in this article are solely those of the authors and do not necessarily represent those of their affiliated

organizations, or those of the publisher, the editors and the reviewers. Any product that may be evaluated in this article, or claim that may be made by its manufacturer, is not guaranteed or endorsed by the publisher.

Supplementary material

The Supplementary Material for this article can be found online at: <https://www.frontiersin.org/articles/10.3389/fendo.2024.1420049/full#supplementary-material>

References

- Kim S, Han S, Kim Y, Kim HS, Gu YR, Kang D, et al. Tankyrase inhibition preserves osteoarthritic cartilage by coordinating cartilage matrix anabolism via effects on SOX9 parylation. *Nat Commun.* (2019) 10:4898. doi: 10.1038/s41467-019-12910-2
- Chimutengwende-Gordon M, Donaldson J, Bentley G. Current solutions for the treatment of chronic articular cartilage defects in the knee. *EFORT Open Rev.* (2020) 5:156–63. doi: 10.1302/2058-5241.5.190031
- Vonk LA, van Dooremalen SFJ, Liv N, Klumperman J, Coffier PJ, Saris DBF, et al. Mesenchymal stromal/stem cell-derived extracellular vesicles promote human cartilage regeneration in vitro. *Theranostics.* (2018) 8:906–20. doi: 10.7150/thno.20746
- Schmitz RJ, Wang HM, Polprasert DR, Kraft RA, Pietrosimone BG. Evaluation of knee cartilage thickness: A comparison between ultrasound and magnetic resonance imaging methods. *Knee.* (2017) 24:217–23. doi: 10.1016/j.knee.2016.10.004
- Akkaya M, Cay N, Gursoy S, Simsek ME, Tahta M, Dogan M, et al. Sonoelastography of the knee joint. *Clin Anat.* (2019) 32:99–104. doi: 10.1002/ca.23300
- Desai P, Hacihaliloglu I. Knee-cartilage segmentation and thickness measurement from 2d ultrasound. *J Imaging.* (2019) 5:43–59. doi: 10.3390/jimaging5040043
- Shi W, Kanamoto T, Aihara M, Oka S, Kuroda S, Nakai T, et al. Articular surface integrity assessed by ultrasound is associated with biological characteristics of articular cartilage in early-stage degeneration. *Sci Rep.* (2022) 12:11970. doi: 10.1038/s41598-022-16248-6
- Ricci V, Ricci C, Gervasoni F, Cocco G, Andreoli A, Özçakar L. From histoanatomy to sonography in myofascial pain syndrome. *Am J Phys Med Rehabil.* (2023) 102:92–7. doi: 10.1097/phm.0000000000001975
- Tamborini G, Hügle T, Ricci V, Filippou G. Ultrasound imaging in crystal arthropathies: A pictorial review. *Reumatismo.* (2023) 75:167–75. doi: 10.4081/reumatismo.2023.1583
- Naredo E, Acebes C, Moller I, Canillas F, de Agustin JJ, de Miguel E, et al. Ultrasound validity in the measurement of knee cartilage thickness. *Ann Rheum Dis.* (2009) 68:1322–7. doi: 10.1136/ard.2008.090738
- Yagi M, Taniguchi M, Tateuchi H, Hirono T, Yamagata M, Umehara J, et al. Relationship between individual forces of each quadriceps head during low-load knee extension and cartilage thickness and knee pain in women with knee osteoarthritis. *Clin Biomech (Bristol Avon).* (2022) 91:105546. doi: 10.1016/j.clinbiomech.2021.105546
- Güvener O, Dağ F, Çimen ÖB, Özçakar L. Ultrasound assessment of distal femoral cartilage thickness measurements of each quadriceps head during walking/jogging in subjects with pes planus. *Knee.* (2022) 39:161–7. doi: 10.1016/j.knee.2022.09.007
- Nieminen HJ, Zheng Y, Saarakkala S, Wang Q, Toyras J, Huang Y, et al. Quantitative assessment of articular cartilage using high-frequency ultrasound: research findings and diagnostic prospects. *Crit Rev BioMed Eng.* (2009) 37:461–94. doi: 10.1615/critrevbiomedeng.v37.i6.20
- Niu HJ, Wang Q, Wang YX, Li DY, Fan YB, Chen WF. Ultrasonic reflection coefficient and surface roughness index of oa articular cartilage: relation to pathological assessment. *BMC Musculoskelet Disord.* (2012) 13:34. doi: 10.1186/1471-2474-13-34
- Sorriento A, Cafarelli A, Valenza G, Ricotti L. Ex-vivo quantitative ultrasound assessment of cartilage degeneration. *Annu Int Conf IEEE Eng Med Biol Soc.* (2021) 2021:2976–80. doi: 10.1109/EMBC46164.2021.9630198
- Lye TH, Gachouch O, Renner L, Elezkurtaj S, Cash H, Messroghli D, et al. Quantitative ultrasound assessment of early osteoarthritis in human articular cartilage using a high-frequency linear array transducer. *Ultrasound Med Biol.* (2022) 48:1429–40. doi: 10.1016/j.ultrasmedbio.2022.03.006
- Deng W, Lin M, Yu S, Liang H, Zhang Z, Liu C. Quantifying region-specific elastic properties of distal femoral articular cartilage: A shear-wave elastography study. *Appl Bionics Biomech.* (2022) 2022:9406863. doi: 10.1155/2022/9406863
- Cay N, Ipek A, Isik C, Unal O, Kartal MG, Arslan H, et al. Strain ratio measurement of femoral cartilage by real-time elastosonography: preliminary results. *Eur Radiol.* (2015) 25:987–93. doi: 10.1007/s00330-014-3497-y
- Everhart JS, Abouljoud MM, Flanigan DC. Role of full-thickness cartilage defects in knee osteoarthritis (Oa) incidence and progression: data from the OA initiative. *J Orthop Res.* (2019) 37:77–83. doi: 10.1002/jor.24140
- Saarakkala S, Toyras J, Hirvonen J, Laasanen MS, Lappalainen R, Jurvelin JS. Ultrasonic quantitation of superficial degradation of articular cartilage. *Ultrasound Med Biol.* (2004) 30:783–92. doi: 10.1016/j.ultrasmedbio.2004.03.005
- Nieminen HJ, Toyras J, Rieppo J, Nieminen MT, Hirvonen J, Korhonen R, et al. Real-time ultrasound analysis of articular cartilage degradation in vitro. *Ultrasound Med Biol.* (2002) 28:519–25. doi: 10.1016/s0301-5629(02)00480-5
- Cherin E, Saied A, Pellaumail B, Loeuille D, Laugier P, Gillet P, et al. Assessment of rat articular cartilage maturation using 50-MHz quantitative ultrasonography. *Osteoarthritis Cartilage.* (2001) 9:178–86. doi: 10.1053/joca.2000.0374
- Liukkonen J, Hirvasniemi J, Joukainen A, Penttilä P, Viren T, Saarakkala S, et al. Arthroscopic ultrasound technique for simultaneous quantitative assessment of articular cartilage and subchondral bone: an in vitro and in vivo feasibility study. *Ultrasound Med Biol.* (2013) 39:1460–8. doi: 10.1016/j.ultrasmedbio.2013.03.026
- Goldring SR. Alterations in periarticular bone and cross talk between subchondral bone and articular cartilage in osteoarthritis. *Ther Adv Musculoskelet Dis.* (2012) 4:249–58. doi: 10.1177/1759720X12437353
- Pritzker KP, Gay S, Jimenez SA, Ostergaard K, Pelletier JP, Revell PA, et al. Osteoarthritis cartilage histopathology: grading and staging. *Osteoarthritis Cartilage.* (2006) 14:13–29. doi: 10.1016/j.joca.2005.07.014
- Wang Y, Guo Y, Zhang L, Niu H, Xu M, Zhao B, et al. Ultrasound biomicroscopy for the detection of early osteoarthritis in an animal model. *Acad Radiol.* (2011) 18:167–73. doi: 10.1016/j.acra.2010.09.011
- Gelse K, Olk A, Eichhorn S, Swoboda B, Schoene M, Raum K. Quantitative ultrasound biomicroscopy for the analysis of healthy and repair cartilage tissue. *Eur Cell Mater.* (2010) 19:58–71. doi: 10.22203/ecm.v019a07
- Kiviranta P, Toyras J, Nieminen MT, Laasanen MS, Saarakkala S, Nieminen HJ, et al. Comparison of novel clinically applicable methodology for sensitive diagnostics of cartilage degeneration. *Eur Cell Mater.* (2007) 13:46–55. doi: 10.22203/ecm.v013a05
- Lisee C, Harkey M, Walker Z, Pfeiffer K, Covassin T, Kovan J, et al. Longitudinal changes in ultrasound-assessed femoral cartilage thickness in individuals from 4 to 6 months following anterior cruciate ligament reconstruction. *Cartilage.* (2021) 13:738S–46S. doi: 10.1177/19476035211038749
- Viren T, Saarakkala S, Jurvelin JS, Pulkkinen HJ, Tiitu V, Valonen P, et al. Quantitative evaluation of spontaneously and surgically repaired rabbit articular cartilage using intra-articular ultrasound method in situ. *Ultrasound Med Biol.* (2010) 36:833–9. doi: 10.1016/j.ultrasmedbio.2010.02.015
- Viren T, Saarakkala S, Tiitu V, Puhakka J, Kiviranta I, Jurvelin J, et al. Ultrasound evaluation of mechanical injury of bovine knee articular cartilage under arthroscopic control. *IEEE Trans Ultrason Ferroelectr Freq Control.* (2011) 58:148–55. doi: 10.1109/TUFFC.2011.1781
- Wang Q, Liu Z, Wang Y, Pan Q, Feng Q, Huang Q, et al. Quantitative ultrasound assessment of cartilage degeneration in ovariectomized rats with low estrogen levels. *Ultrasound Med Biol.* (2016) 42:290–8. doi: 10.1016/j.ultrasmedbio.2015.08.004
- Huang YP, Zhong J, Chen J, Yan CH, Zheng YP, Wen CY. High-frequency ultrasound imaging of tidemark in vitro in advanced knee osteoarthritis. *Ultrasound Med Biol.* (2018) 44:94–101. doi: 10.1016/j.ultrasmedbio.2017.08.1884
- Zhang J, Xiao L, Tong L, Wan C, Hao Z. Quantitative evaluation of enzyme-induced porcine articular cartilage degeneration based on observation of entire cartilage layer using ultrasound. *Ultrasound Med Biol.* (2018) 44:861–71. doi: 10.1016/j.ultrasmedbio.2017.11.016
- Pastrama M, Spierings J, van Hugten P, Ito K, Lopata R, van Donkelaar CC. Ultrasound-based quantification of cartilage damage after in vivo articulation with metal implants. *Cartilage.* (2021) 13:1540S–50S. doi: 10.1177/19476035211063861

36. Ozturk A, Grajo JR, Dhyani M, Anthony BW, Samir AE. Principles of ultrasound elastography. *Abdom Radiol (NY)*. (2018) 43:773–85. doi: 10.1007/s00261-018-1475-6
37. Gennisson JL, Defieux T, Fink M, Tanter M. Ultrasound elastography: principles and techniques. *Diagn Interv Imaging*. (2013) 94:487–95. doi: 10.1016/j.diii.2013.01.022
38. Shiina T. Wfumb guidelines and recommendations for clinical use of ultrasound elastography: part 1: basic principles and terminology. *Ultrasound Med Biol*. (2017) 43: S191–S2. doi: 10.1016/j.ultrasmedbio.2017.08.1653
39. Cui XW, Li KN, Yi AJ, Wang B, Wei Q, Wu GG, et al. Ultrasound elastography. *Endosc Ultrasound*. (2022) 11:252–74. doi: 10.4103/EUS-D-21-00151
40. Li J, Chen M, Cao CL, Zhou LQ, Li SG, Ge ZK, et al. Diagnostic performance of acoustic radiation force impulse elastography for the differentiation of benign and malignant superficial lymph nodes: A meta-analysis. *J Ultrasound Med*. (2020) 39:213–22. doi: 10.1002/jum.15096
41. Ignee A, Jenssen C, Arcidiacono PG, Hocke M, Moller K, Saftou A, et al. Endoscopic ultrasound elastography of small solid pancreatic lesions: A multicenter study. *Endoscopy*. (2018) 50:1071–9. doi: 10.1055/a-0588-4941
42. Dong Y, D'Onofrio M, Hocke M, Jenssen C, Potthoff A, Atkinson N, et al. Autoimmune pancreatitis: imaging features. *Endosc Ultrasound*. (2018) 7:196–203. doi: 10.4103/eus.eus_23_17
43. Aslan A, Barutca H, Ayaz E, Aslan M, Kocaaslan C, Inan I, et al. Is real-time elastography helpful to differentiate acute from subacute deep venous thrombosis? A preliminary study. *J Clin Ultrasound*. (2018) 46:116–21. doi: 10.1002/jcu.22522
44. Wang B, Guo Q, Wang JY, Yu Y, Yi AJ, Cui XW, et al. Ultrasound elastography for the evaluation of lymph nodes. *Front Oncol*. (2021) 11:714660. doi: 10.3389/fonc.2021.714660
45. Wadugodapitiya S, Sakamoto M, Tanaka M, Sakagami Y, Morise Y, Kobayashi K. Assessment of knee collateral ligament stiffness by strain ultrasound elastography. *BioMed Mater Eng*. (2022) 33:337–49. doi: 10.3233/BME-211282
46. Sahan MH, Bayar Muluk N, Inal M, Asal N, Simsek G, Arikani OK. Sonoelastographic evaluation of the lower lateral nasal cartilage lateral crus, auricular conchal cartilage, and costal cartilage. *Facial Plast Surg*. (2019) 35:678–86. doi: 10.1055/s-0039-3399577
47. Ferraioli G, Roccarina D. Update on the role of elastography in liver disease. *Therap Adv Gastroenterol*. (2022) 15:17562848221140657. doi: 10.1177/17562848221140657
48. Ruan SM, Huang H, Cheng MQ, Lin MX, Hu HT, Huang Y, et al. Shear-wave elastography combined with contrast-enhanced ultrasound algorithm for noninvasive characterization of focal liver lesions. *Radiol Med*. (2023) 128:6–15. doi: 10.1007/s11547-022-01575-5
49. Zhang Y, Lu F, Shi H, Guo LH, Wei Q, Xu HX, et al. Predicting Malignancy in thyroid nodules with benign cytology results: the role of conventional ultrasound, shear wave elastography and braf V600e. *Clin Hemorheol Microcirc*. (2022) 81:33–45. doi: 10.3233/CH-211337
50. Han R, Li F, Wang Y, Ying Z, Zhang Y. Virtual touch tissue quantification (Vtq) in the diagnosis of thyroid nodules with coexistent chronic autoimmune hashimoto's thyroiditis: A preliminary study. *Eur J Radiol*. (2015) 84:327–31. doi: 10.1016/j.ejrad.2014.11.005
51. Cong Y, Fan Z, Dai Y, Zhang Z, Yan K. Application value of shear wave elastography in the evaluation of tumor downstaging for locally advanced rectal cancer after neoadjuvant chemoradiotherapy. *J Ultrasound Med*. (2021) 40:81–9. doi: 10.1002/jum.15378
52. Lee S, Eun LY, Hwang JY, Eun Y. Ex vivo evaluation of mechanical anisotropic tissues with high-frequency ultrasound shear wave elastography. *Sensors (Basel)*. (2022) 22:978–93. doi: 10.3390/s22030978
53. Stiver ML, Mirjalili SA, Agur AMR. Measuring shear wave velocity in adult skeletal muscle with ultrasound 2-D shear wave elastography: A scoping review. *Ultrasound Med Biol*. (2023) 49:1353–62. doi: 10.1016/j.ultrasmedbio.2023.02.005
54. Cloutier G, Cardinal MR, Ju Y, Giroux MF, Lanthier S, Soulez G. Carotid plaque vulnerability assessment using ultrasound elastography and echogenicity analysis. *AJR Am J Roentgenol*. (2018) 211:847–55. doi: 10.2214/AJR.17.19211
55. Chandra L, Ortiz J, Weitzel W, Hamilton JD, Gao J. Ultrasound elastography detects age-related changes in adult false vocal folds. *J Ultrasound Med*. (2023) 42:575–83. doi: 10.1002/jum.16033
56. Yin L, Du L, Li Y, Xiao Y, Zhang S, Ma H, et al. Quantitative evaluation of gastrocnemius medialis stiffness during passive stretching using shear wave elastography in patients with parkinson's disease: A prospective preliminary study. *Korean J Radiol*. (2021) 22:1841–9. doi: 10.3348/kjr.2020.1338
57. Sernik RA, Pereira RFB, Cerri GG, Damasceno RS, Bastos BB, Leao RV. Shear wave elastography is a valuable tool for diagnosing and grading carpal tunnel syndrome. *Skeletal Radiol*. (2023) 52:67–72. doi: 10.1007/s00256-022-04143-0
58. Huang M, Miller T, Fu SN, Ying MTC, Pang MYC. Structural and passive mechanical properties of the medial gastrocnemius muscle in ambulatory individuals with chronic stroke. *Clin Biomech (Bristol Avon)*. (2022) 96:105672. doi: 10.1016/j.clinbiomech.2022.105672
59. Gurun E, Akdulm I, Akyuz M, Oktar SO. Shear wave elastography evaluation of brachial plexus in multiple sclerosis. *Acta Radiol*. (2022) 63:520–6. doi: 10.1177/02841851211002828
60. Kohli DR, Mettman D, Andraws N, Haer E, Porter J, Ulusurac O, et al. Comparative accuracy of endosonographic shear wave elastography and transcutaneous liver stiffness measurement: A pilot study. *Gastrointest Endosc*. (2023) 97:35–41.e1. doi: 10.1016/j.gie.2022.08.035
61. Wang T, Jirapinyo P, Shah R, Schuster K, Thompson C, Lautz D, et al. Endoscopic ultrasound shear wave elastography is superior to fibroscan and non-invasive scores for fibrosis staging in patients with obesity and non-alcoholic fatty liver disease: A true virtual biopsy. *Gastrointestinal Endoscopy*. (2023) 97:AB787–AB8. doi: 10.1016/j.gie.2023.04.1286
62. Ivanochko NK, Gatti AA, Stratford PW, Maly MR. Interactions of cumulative load with biomarkers of cartilage turnover predict knee cartilage change over 2 years: data from the osteoarthritis initiative. *Clin Rheumatol*. (2024) 43:2317–27. doi: 10.1007/s10067-024-07014-2
63. Dreiner M, Willwacher S, Kramer A, Kümmel J, Frett T, Zaucke F, et al. Short-term response of serum cartilage oligomeric matrix protein to different types of impact loading under normal and artificial gravity. *Front Physiol*. (2020) 11:1032. doi: 10.3389/fphys.2020.01032
64. Brenneman Wilson EC, Gatti AA, Keir PJ, Maly MR. Daily cumulative load and body mass index alter knee cartilage response to running in women. *Gait Posture*. (2021) 88:192–7. doi: 10.1016/j.gaitpost.2021.05.030
65. Hatta T, Giambini H, Sukegawa K, Yamanaka Y, Sperling JW, Steinmann SP, et al. Quantified mechanical properties of the deltoid muscle using the shear wave elastography: potential implications for reverse shoulder arthroplasty. *PLoS One*. (2016) 11:e0155102. doi: 10.1371/journal.pone.0155102
66. Akkaya S, Akkaya N, Gungor HR, Agladioglu K, Ok N, Ozcakar L. Sonoelastographic evaluation of the distal femoral cartilage in patients with anterior cruciate ligament reconstruction. *Eklemler Hastalik Cerrahisi*. (2016) 27:2–8. doi: 10.5606/ehc.2016.02
67. Yokus A, Toprak M, Arslan H, Toprak N, Akdeniz H, Gunduz AM. Evaluation of distal femoral cartilage by B-mode ultrasonography and shear wave elastography in patients with knee osteoarthritis: A preliminary study. *Acta Radiol*. (2021) 62:510–4. doi: 10.1177/0284185120930642
68. Zhang X, Lin D, Jiang J, Guo Z. Preliminary study on grading diagnosis of early knee osteoarthritis by shear wave elastography. *Contrast Media Mol Imaging*. (2022) 2022:4229181. doi: 10.1155/2022/4229181
69. Filippucci E, da Luz KR, Di Geso L, Salaffi F, Tardella M, Carotti M, et al. Interobserver reliability of ultrasonography in the assessment of cartilage damage in rheumatoid arthritis. *Ann Rheum Dis*. (2010) 69:1845–8. doi: 10.1136/ard.2009.125179
70. Pradsgaard DO, Fiirgaard B, Spannow AH, Heuck C, Herlin T. Cartilage thickness of the knee joint in juvenile idiopathic arthritis: comparative assessment by ultrasonography and magnetic resonance imaging. *J Rheumatol*. (2015) 42:534–40. doi: 10.3899/jrheum.140162
71. Jain S, Khanduri S, Khan M, Khan S, Yadav VK, Khan BR, et al. Mid-second trimester measurement of nasal bone length in North Indian population. *J Clin Imaging Sci*. (2019) 9:14. doi: 10.25259/JCIS-15-2019
72. Arjunan SP, Thomas MC. A review of ultrasound imaging techniques for the detection of down syndrome. *Irbm*. (2020) 41:115–23. doi: 10.1016/j.irbm.2019.10.004
73. Aisen AM, McCune WJ, MacGuire A, Carson PL, Silver TM, Jafri SZ, et al. Sonographic evaluation of the cartilage of the knee. *Radiology*. (1984) 153:781–4. doi: 10.1148/radiology.153.3.6387794
74. Disler DG, Raymond E, May DA, Wayne JS, McCauley TR. Articular cartilage defects: *in vitro* evaluation of accuracy and interobserver reliability for detection and grading with us. *Radiology*. (2000) 215:846–51. doi: 10.1148/radiology.215.3.r00jn20846
75. Devrimsel G, Beyazal MS, Turkyilmaz AK, Sahin SB. Ultrasonographic evaluation of the femoral cartilage thickness in patients with hypothyroidism. *J Phys Ther Sci*. (2016) 28:2249–52. doi: 10.1589/jpts.28.2249
76. Fiorentino MC, Cipolletta E, Filippucci E, Grassi W, Frontoni E, Moccia S. A deep-learning framework for metacarpal-head cartilage-thickness estimation in ultrasound rheumatological images. *Comput Biol Med*. (2022) 141:105117. doi: 10.1016/j.cmpbiomed.2021.105117
77. Faisal A, Ng SC, Goh SL, Lai KW. Knee cartilage segmentation and thickness computation from ultrasound images. *Med Biol Eng Comput*. (2018) 56:657–69. doi: 10.1007/s11517-017-1710-2
78. Zatloukalova J, Raum K. High frequency ultrasound assesses transient changes in cartilage under osmotic loading. *Math Biosci Eng*. (2020) 17:5190–211. doi: 10.3934/mbe.2020281
79. Pirri C, Stecco C, Güvener O, Mezian K, Ricci V, Jačisko J, et al. Euro-musculus/usprm dynamic ultrasound protocols for knee. *Am J Phys Med Rehabil*. (2023) 102:e67–72. doi: 10.1097/pbm.0000000000002173
80. Mezian K, Ricci V, Güvener O, Jačisko J, Novotný T, Kara M, et al. Euro-musculus/usprm dynamic ultrasound protocols for (Adult) hip. *Am J Phys Med Rehabil*. (2022) 101:e162–e8. doi: 10.1097/pbm.0000000000002061
81. Okada S, Taniguchi M, Yagi M, Motomura Y, Okada S, Fukumoto Y, et al. Ultrasonographic echo intensity in the medial femoral cartilage is enhanced prior to cartilage thinning in women with early mild knee osteoarthritis. *Knee Surg Sports Traumatol Arthrosc*. (2023) 31:3964–70. doi: 10.1007/s00167-023-07440-w
82. Okada S, Taniguchi M, Yagi M, Motomura Y, Okada S, Nakazato K, et al. Characteristics of acute cartilage response after mechanical loading in patients with

early-mild knee osteoarthritis. *Ann BioMed Eng.* (2024) 52:1326–34. doi: 10.1007/s10439-024-03456-6

83. Printemps C, Cousin I, Le Lez Soquet S, Saliou P, Josse A, De Vries P, et al. Pulvinar and pubic cartilage measurements to refine universal ultrasound screening for developmental dysplasia of the hip: data from 1896 infant hips. *Eur J Radiol.* (2021) 139:109727. doi: 10.1016/j.ejrad.2021.109727

84. Harkey MS, Blackburn JT, Davis H, Sierra-Arevalo L, Nissman D, Pietrosimone B. Ultrasonographic assessment of medial femoral cartilage deformation acutely following walking and running. *Osteoarthritis Cartilage.* (2017) 25:907–13. doi: 10.1016/j.joca.2016.12.026

85. Yildirim A, Onder ME, Ozkan D. Ultrasonographic evaluation of distal femoral and talar cartilage thicknesses in patients with early rheumatoid arthritis and their relationship with disease activity. *Clin Rheumatol.* (2022) 41:2001–7. doi: 10.1007/s10067-022-06132-z

86. Moller B, Bonel H, Rotzetter M, Villiger PM, Ziswiler HR. Measuring finger joint cartilage by ultrasound as a promising alternative to conventional radiograph imaging. *Arthritis Rheum.* (2009) 61:435–41. doi: 10.1002/art.24424

87. Kaya A, Kara M, Tiftik T, Tezcan ME, Ozturk MA, Akinci A, et al. Ultrasonographic evaluation of the femoral cartilage thickness in patients with systemic lupus erythematosus. *Rheumatol Int.* (2013) 33:899–901. doi: 10.1007/s00296-012-2462-9